

Neuronal Dynamics Underlying High- and Low-Frequency EEG Oscillations Contribute Independently to the Human BOLD Signal

René Scheeringa,^{1,2,*} Pascal Fries,^{1,3} Karl-Magnus Petersson,^{1,4} Robert Oostenveld,¹ Iris Grothe,^{1,5,6} David G. Norris,¹ Peter Hagoort,^{1,4} and Marcel C.M. Bastiaansen^{1,4}

¹Donders Institute for Brain Cognition and Behaviour, Centre for Cognitive Neuroimaging, Radboud University Nijmegen, 6500 HB Nijmegen, The Netherlands

²Cognitive Neuro-Imaging Unit, Institut National de la Santé et de la Recherche Médicale, Neurospin, Commissariat à l'Énergie Atomique, 91190 Gif sur Yvette, France

³Ernst Strüngmann Institute (ESI) in Cooperation with Max Planck Society, D-60528 Frankfurt, Germany

⁴Max Planck Institute for Psycholinguistics, 6500 AH Nijmegen, The Netherlands

⁵Institute for Brain Research, Department of Theoretical Neurobiology, University of Bremen, D-28359 Bremen, Germany

⁶Center for Cognitive Sciences, University of Bremen, D-28359 Bremen, Germany

*Correspondence: rene.scheeringa@donders.ru.nl

DOI 10.1016/j.neuron.2010.11.044

SUMMARY

Work on animals indicates that BOLD is preferentially sensitive to local field potentials, and that it correlates most strongly with gamma band neuronal synchronization. Here we investigate how the BOLD signal in humans performing a cognitive task is related to neuronal synchronization across different frequency bands. We simultaneously recorded EEG and BOLD while subjects engaged in a visual attention task known to induce sustained changes in neuronal synchronization across a wide range of frequencies. Trial-by-trial BOLD fluctuations correlated positively with trial-by-trial fluctuations in high-EEG gamma power (60–80 Hz) and negatively with alpha and beta power. Gamma power on the one hand, and alpha and beta power on the other hand, independently contributed to explaining BOLD variance. These results indicate that the BOLD-gamma coupling observed in animals can be extrapolated to humans performing a task and that neuronal dynamics underlying high- and low-frequency synchronization contribute independently to the BOLD signal.

INTRODUCTION

Functional magnetic resonance imaging (fMRI) is now the most widely used research tool in human cognitive neuroscience. In this branch of science, the hemodynamic responses obtained with fMRI measurements are commonly used to infer relationships between brain activity and cognitive functions. However, the exact relation between hemodynamic responses as measured with fMRI blood-oxygenation-level-dependent (BOLD) responses on the one hand, and underlying neuronal activity on the other, is

not fully understood (Logothetis, 2008). Recordings in both the anesthetized and awake monkey have shown that hemodynamic responses are preferentially sensitive to local field potentials (LFP) as opposed to action potentials (Goense and Logothetis, 2008; Logothetis et al., 2001). In addition, recordings from anesthetized cat visual cortex have revealed a strong positive correlation between BOLD and neuronal synchronization in the gamma frequency range (>30 Hz) together with a negative correlation of BOLD with lower frequency bands (up to 7 Hz) (Niessing et al., 2005). However, in order for these results to have validity for fMRI studies in human cognitive neuroscience, an important question is how changes in neural synchronization across different frequency bands are related to changes in the BOLD signal in humans performing a cognitive task. We therefore seek to replicate the positive correlation between high-gamma power and the BOLD signal found in animals in humans performing a cognitive task and to investigate whether contributions to the BOLD signal related to high-frequency synchronization are independent from the contributions related to low-frequency desynchronization.

Most studies with simultaneous EEG and fMRI have reported negative correlations with BOLD in the low-frequency ranges (roughly 4–30 Hz) of the spectrum (Goldman et al., 2002; Laufs et al., 2003a; Scheeringa et al., 2008, 2009; Yuan et al., 2010). Concerning the high-gamma frequency range, encouraging first findings in this context are that the reactivity patterns of human and monkey gamma band oscillations appear to show strong similarity, at least in the visual cortex (Fries et al., 2008; Hall et al., 2005). Furthermore there is some evidence suggesting that gamma range fluctuations in electrophysiological recordings are also closely related to the BOLD signal in humans. Single-unit recordings of spike trains and high-frequency LFPs in the auditory cortex of patients watching a movie correlated significantly with fMRI BOLD responses measured in another set of healthy volunteers watching the same movie (Mukamel et al., 2005). Separate recordings of intracranial EEG and fMRI during a semantic decision task showed close spatial correspondence between regions of fMRI activations and EEG

recording sites showing task effects in the high-gamma range. A recent simultaneous EEG-fMRI study reported a positive correlation between low-range (~40 Hz) gamma band power and primary auditory cortex in an auditory task (Mulert et al., 2010). Furthermore, a study with an adapted version of the task used in our study reported that task-related parametric modulations in gamma power correspond well with parametric modulations in the NIRS signal, which was used as a hemodynamic measure (Koch et al., 2009).

In light of this previous work, we set out to study the relation between the BOLD signal and electrophysiological power changes across a broad frequency spectrum for humans performing a cognitive task. We therefore asked subjects to engage in a visual attention task known to elicit strong, long-lasting (up to several seconds) increases in rhythmic activity in a relatively narrow high-gamma frequency band as well as decreases in the alpha and beta band oscillations in the MEG (Hoogenboom et al., 2006) and EEG (Fries et al., 2008). From this previous work we know that in this task both increases in gamma power and decreases in alpha and beta power originate from early visual cortices. This task is therefore well suited for studying the relationship between frequency-specific power changes in the scalp EEG on the one hand and simultaneously measured fMRI BOLD changes on the other hand. Moreover, the narrow-band high-gamma increase found in this task has been observed in human EEG and MEG data as well as monkey LFP data (Fries et al., 2008) and therefore provides a good link with animal work.

We hypothesized a positive correlation between BOLD and EEG gamma power in parallel to what has been observed in animal experiments. In addition, we also explored the relationship between BOLD and other lower EEG frequency bands, in order to establish whether the negative correlation between BOLD and lower frequency neuronal synchronization observed previously independently contributes to explaining BOLD variance.

RESULTS

Standard EEG and fMRI Analysis

To study the relation between frequency-specific EEG power and the BOLD fMRI signal, we used a visual attention task in which subjects had to detect a speed increase in inward-moving circular sinusoidal gratings (see Figure 1). After applying an independent component analysis (ICA) denoising strategy (see Experimental Procedures), visually induced power changes in the EEG recorded in the MR revealed a decrease in alpha (~10 Hz) and beta (~20 Hz) power together with an increase in gamma (60–80 Hz) power. Time-frequency representations of the results are shown in Figure 2A and scalp topographies of the time-frequency effects are shown in Figure 2B. A standard analysis of the fMRI data shows BOLD activations in the early visual cortex (Figure 2C). The locations of the BOLD activations correspond well with the scalp topographies of the EEG responses (Figure 2B) and estimated source localization in MEG by using the same task (Hoogenboom et al., 2006). The reported EEG and fMRI effects were highly consistent across subjects (see Figure S1, available online) and the EEG effects are very similar to those obtained with MEG and EEG measurements outside the MR scanner by using adapted versions of the

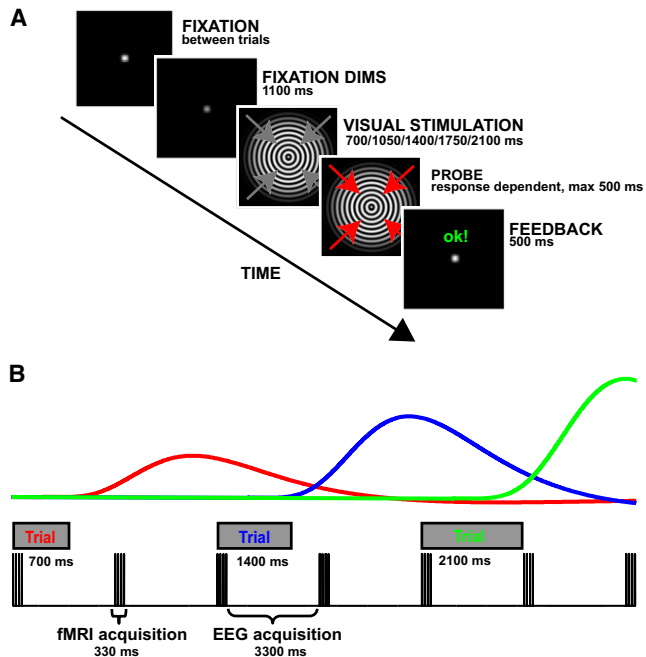


Figure 1. Schematic Representation of the Task

(A) Sequence of events of a single trial. A trial started at the beginning of the acquisition of an fMRI volume with the reduction of the contrast of the fixation dot (the warning signal). After 1100 ms the fixation point is replaced by a foveal contracting grating, with a duration of either 700, 1050, 1400, 1750, or 2100 ms. Except for the 2100 ms condition (catch trials), visual stimulation was followed by an increase in the speed of the foveal contraction. Subjects were instructed to push a button as soon as they detected the speed change. Subsequently, feedback was presented for 500 ms.

(B) Illustration of the timing of the trials relative to fMRI data acquisition. Trials were presented every two volumes. Scanning parameters were chosen such that the visual stimulation part of the trial would always be outside the fMRI acquisition, allowing for good quality EEG acquisition. As illustrated by the canonical HRFs to the visual stimulation of different lengths, the second fMRI volume after stimulation onset is close to the expected peak of the BOLD response. Trials of different lengths were modeled with separate regressors.

same task used here (Hoogenboom et al., 2006; Koch et al., 2009).

Joint EEG-fMRI Analysis

In order to test for a more direct link between hemodynamic responses and human gamma band activity, we set up a statistical model that evaluates whether trial-by-trial fluctuations in BOLD covary with trial-by-trial fluctuations in frequency-specific EEG power.

We constructed separate design matrices for each individual frequency bin in the EEG signal, from 2.5 to 120 Hz. Each of these design matrices included a frequency-specific regressor based on the single-trial EEG power estimates, as well as a set of regressors modeling the task and reaction time (separate regressors for each trial length). The average BOLD signal in the single-subject activations in early visual cortex for the standard fMRI analysis was used as the dependent variable.

Investigating frequencies up to 120 Hz produces a spectrum of beta values. Since beta values can differ by orders of

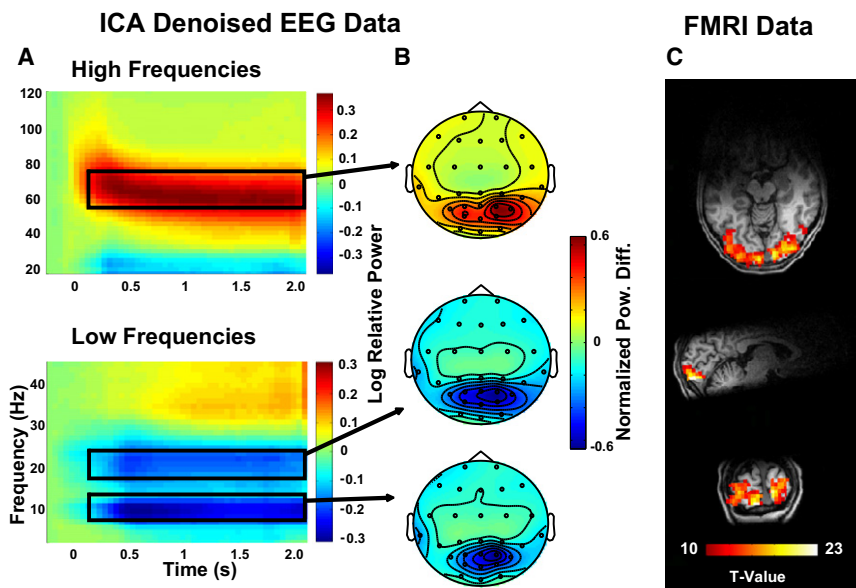


Figure 2. Results for EEG and fMRI Data

(A) The grand average time-frequency representations (TFRs) are shown of log-transformed EEG power for low and high frequencies after back reconstruction of the selected components to channel level. ICA unmixing weights were estimated on individual gamma-band-filtered EEG data. This grand average is based on individual averages of the channels that formed the regressors in the integrated EEG fMRI analysis.

(B) The grand average topographies of the alpha, beta, and gamma effects are shown, computed as the average over individual power differences normalized to the maximum of the absolute difference in the indicated frequency bands.

(C) The BOLD activations for a representative subject are shown. Individual TFRs and BOLD activation plots are presented in Figure S1. The TFRs and topographies obtained by applying ICA on 30 Hz low-pass-filtered data are shown in Figure S2.

magnitude between frequencies and subjects, they were converted to *t* values in order to express the strength of the relation between EEG power and the BOLD signal. Separate spectra for the low (<45 Hz) and high (10–120 Hz) frequencies were constructed with different spectral concentrations (see [Experimental Procedures](#) for details and rationale). The results of this analysis are shown in Figure 3. There is a significant positive relation between BOLD and EEG gamma power in the 60–80 Hz frequency range ($p = 0.004$, corrected for multiple comparisons) and a negative relation between BOLD and low-frequency EEG power in the alpha frequency range (~10 Hz; $p = 0.030$) and in the beta frequency range (18–28 Hz; $p = 0.002$). In addition, there is a marked correspondence between the BOLD-EEG correlation spectrum on the one hand and the spectral changes observed in the EEG compared to a baseline 200 ms before the onset of the visual stimulation (compare Figures 3A and 3B with Figures 3C and 3D).

In order to test whether the three observed frequency effects in the EEG are independent of each other, we tested a general linear model (GLM) that included regressors modeling the EEG alpha, beta, and gamma power fluctuations. These regressors therefore account for a unique part of the variance of the BOLD signal, whereas variance that can be explained by more than one band is excluded for each regressor. The results are compared with models in which only one EEG-based regressor is included. The analysis (Figure 3E) shows that the alpha band only marginally contributes to explaining BOLD variance on its own. The beta band contribution is reduced but significant, whereas trial-by-trial fluctuations unique for the gamma band most strongly and significantly contribute to explaining BOLD variance. A pairwise partial correlation (correcting for mean task and reaction-time regressors) of these EEG power regressors (Figure 3F) shows why this pattern emerges. While alpha and beta regressors show a significant positive correlation, they both do not correlate with gamma power. Thus, while the trial-by-trial power fluctuations in the alpha and beta regressors

are highly correlated with each other, those in the gamma regressor are independent from the trial-by-trial fluctuations of power in these low-frequency bands.

For seven subjects a clear sustained lower gamma band increase was detected. For these subjects an additional analysis was carried out by using a subject-specific low-gamma band regressor (see [Experimental Procedures](#) for details). The trial-by-trial relation between BOLD and low gamma is depicted in Figure 4. For comparison, the effects in the alpha, beta, and high-gamma band are also depicted for these seven subjects. This analysis revealed a positive relation ($p = 0.047$ uncorrected, Wilcoxon ranked sign test; [Wilcoxon, 1945](#)) between BOLD and low-gamma power. This should be interpreted as a clear trend, since no correction for multiple comparisons was applied, but on the other hand it is based on only a few subjects.

Infraslow Fluctuations

Several studies have demonstrated that the phase of slow (<4 Hz) and infraslow electrophysiological fluctuations (roughly <0.1 Hz) modulate the amplitude across a wide range of higher frequencies ([He et al., 2010](#); [Monto et al., 2008](#)). Especially these infraslow oscillations are also thought to be related to the changes in the BOLD signal ([He et al., 2008](#); [Nir et al., 2008](#)), because both act on similar timescales. This therefore raises the question whether the trial-by-trial relation between BOLD and EEG power in the alpha, beta, and gamma bands we observed is related to these infraslow oscillations. We investigated this by calculating the coherence spectrum between trial-by-trial fluctuations in both BOLD and EEG power for the same frequencies used in creating the BOLD-EEG correlation spectra (Figures 3C and 3D). This results in a two-dimensional image that depicts in a frequency-resolved manner how changes in frequency-specific EEG power are related to the BOLD signal (see Figure 5). If infraslow oscillations influence the relation between BOLD and EEG power at higher frequencies, this should be reflected in increased BOLD-EEG power coherence in the infraslow frequency range.

In general, this analysis revealed elevated coherence for EEG frequency ranges that were also observed in the BOLD-EEG correlational approach (Figure 5A). An exception can be found in the theta range (3–7 Hz), which is continuous with elevated coherence in the alpha range. Figure 5B depicts the phase of the coherence and shows that the clusters of elevated coherence in the low-frequency ranges have a phase near π or $-\pi$, which indicates that the BOLD signal and the EEG power regressors are coupled in antiphase for these frequencies. For the elevated coherence in the high-gamma range, phase values near zero are observed, which indicates that BOLD and EEG power regressors are in phase for these frequencies. This pattern corresponds with the negative BOLD-EEG correlation observed in the alpha and beta bands and positive correlations observed in the gamma band.

If we assess the coherence profiles of the different EEG frequency bands in more detail, different coherence profiles can be observed for the alpha, beta, and gamma bands for which a significant EEG-BOLD correlation was detected. For the alpha and low-beta range increased coherence is observed at the higher end of the coherence spectrum (>0.11 Hz). This is close to the trial rate of 0.138 Hz, and therefore the inverse relations between alpha and low beta and BOLD probably are not modulated by infraslow oscillations. For the higher beta EEG power range (>20 Hz) elevated coherence is more broadly distributed between 0.05 and 0.1 Hz, which could be regarded as the high end of the ultraslow range. In the gamma range between 60 and 80 Hz a different coherence profile can be observed. Similar to the alpha and beta bands, elevated coherence in this range can be observed in the high end of the coherence spectrum (>0.12 Hz). A clear difference with these bands, however, is that elevated coherence is also observed in the very low end of the coherence spectrum (<0.02 Hz). This indicates that both very slow and relatively fast fluctuations over trials in the gamma response are related to the BOLD signal. These findings support the notion that infraslow oscillations are coupled to higher frequency power changes and their relation to the BOLD signal. The elevated coherence near the trial-rate frequency, however, indicates that these fluctuations in the ultraslow range are not the only source of trial-by-trial coupling between BOLD and EEG power in higher frequencies.

DISCUSSION

We aimed to investigate (1) how changes in neural synchronization in different frequency bands are related to BOLD changes in humans performing a cognitive task and (2) whether the neuronal dynamics underlying the different frequency bands contribute independently to the BOLD signal. We found that in human early visual cortex during an attentional monitoring task, trial-by-trial BOLD fluctuations correlated positively with simultaneously recorded trial-by-trial fluctuations in narrow-band high frequency (60–80 Hz) and probably also low-frequency (30–45 Hz) EEG gamma power. In addition, BOLD fluctuations correlated negatively with EEG alpha and beta power. The neural processes underlying high-gamma power on the one hand and alpha and beta power on the other hand independently contributed to explaining BOLD variance.

It is a frequently observed phenomenon that functional activation of a brain region leads to enhanced high-frequency power and reduced low-frequency power. This is also what we observe in our data (Figures 2A and 2B and Figures 3A and 3B): In response to the visual stimulation there is a strong decrease in the alpha and beta bands and a strong increase in the high-gamma band. This raises the question of how alpha and beta on the one hand and high gamma on the other can independently contribute to explaining BOLD variance. This question can be answered by realizing that instead of considering EEG power as such, our present work focuses on how trial-by-trial variability in different frequency bands is related to trial-by-trial variability in the BOLD signal. Crucially, we show (Figure 3F) that the trial-by-trial fluctuations in alpha and beta power on the one hand and in high-gamma power on the other hand, are uncorrelated, though both contribute to the BOLD response. This strongly suggests that these contributions are independent from each other.

Furthermore, the trial-by-trial correlation between alpha and beta power on the one hand, and high gamma on the other, is assessed after convolution with a hemodynamic response function, which has the property of acting as a low-pass filter. This implies that high-frequency fluctuations of power in alpha and beta and high-gamma bands might still be dependent. These faster power fluctuations, however, cannot contribute to the neural influence on the BOLD signal, which is low frequency in nature. Finally, the BOLD-EEG coherence analysis further strengthens the notion that alpha and beta on the one hand, and high gamma on the other hand, independently contribute to explaining BOLD variance: the BOLD-gamma coupling is modulated by very slow oscillations (<0.02 Hz), while the BOLD-alpha and BOLD-beta coupling are not (Figure 5).

Taken together, our results indicate that, apart from high-gamma band neuronal synchronization, another independent mechanism underlying hemodynamic responses is inversely related to neuronal dynamics in the lower (alpha and beta) frequency ranges. This is consistent with previous work that established a negative correlation between fMRI BOLD activations and low-frequency (4–30 Hz) neuronal synchronization (Goldman et al., 2002; Laufs et al., 2003a, 2006; Mukamel et al., 2005; Niessing et al., 2005; Scheeringa et al., 2008, 2009; Yuan et al., 2010). The interdependence of alpha band and beta band power fluctuations suggests that neuronal dynamics in these two frequency ranges are related. Although this would fit the observation that event-related changes in alpha and beta rhythms often co-occur, e.g., during self-paced movements (Pfurtscheller et al., 1996a, 1996b), these rhythms are often considered to subservise different (though not very consistently specified) functions (Jokisch and Jensen, 2007; Klimesch et al., 1998, 2007; Palva and Palva, 2007; Posthuma et al., 2001). An important implication of our observations is that alpha and beta rhythms contribute to explaining BOLD variance independently of high-gamma band dynamics.

Low- and high-frequency oscillations might also be brought about by different mechanisms. By using cell-type-specific optogenetic activation, Cardin and colleagues (Cardin et al., 2009) were able to show a cell-type-specific double dissociation. Whereas rhythmic driving of fast-spiking interneurons selectively increased gamma band LFP power, the rhythmic driving of the

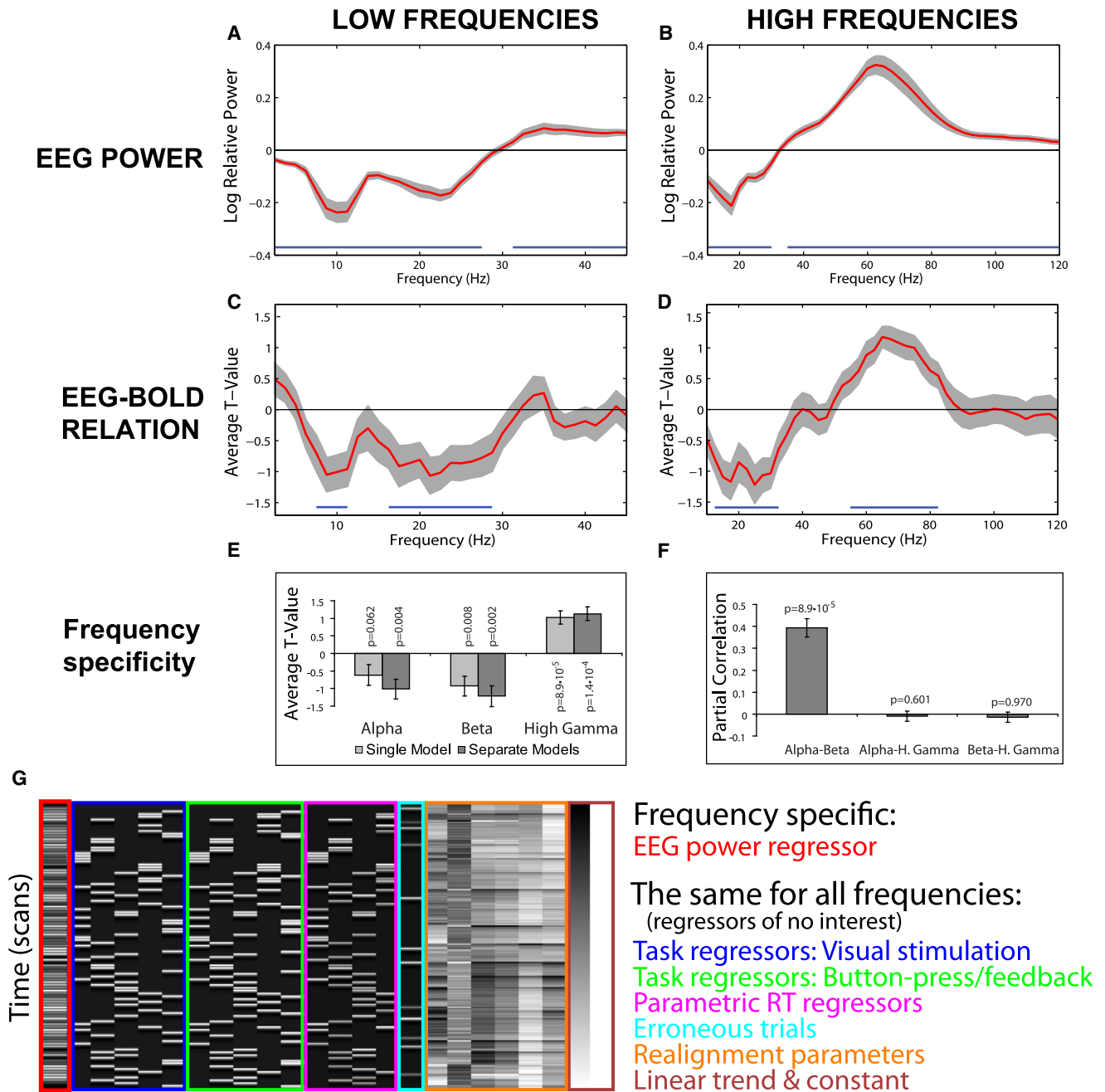


Figure 3. BOLD-EEG Power Correlations

(A and B) Spectra of the group average of the log-transformed relative power effects compared to a prestimulation baseline for low and high frequencies. Prior to averaging over subjects, the spectra were averaged over the visual stimulation part of the trial and the same channels that were selected for regressor construction. The frequencies between 2.5 and 45 Hz in 1.25 Hz steps are depicted in (A). Each frequency bin integrates the power in a 5 Hz window (± 2.5 Hz). The frequencies between 10 and 120 Hz in 2.5 Hz steps are depicted in (B). Each frequency bin integrates the power in a 20 Hz window (± 10 Hz).

(C and D) Relation between trial-by-trial fluctuations in BOLD and EEG power for low and high frequencies expressed in averaged t-values. The frequency resolution in (C) and (D) is the same as for (A) and (B), respectively. The gray shaded area in (A)–(D) indicates the standard error of the mean; a blue line indicates a significant deviation from zero with a cluster-based randomization technique (Maris and Oostenveld, 2007). The results of a similar analysis after applying ICA on 30 Hz low-pass-filtered EEG data are shown in Figure S2.

(E) Average t-values are shown of one general linear model that included regressors modeling alpha, beta, and gamma power fluctuations in the same design matrix and of separate models including only one EEG power regressor.

(F) The partial correlation between the alpha, beta, and gamma regressors is shown. The regressors modeling the visual stimulation, button presses and feedback, and RT were separated out. The error bars in (E) and (F) indicate the standard error of the mean and the p-values are based on the Wilcoxon ranked sign test.

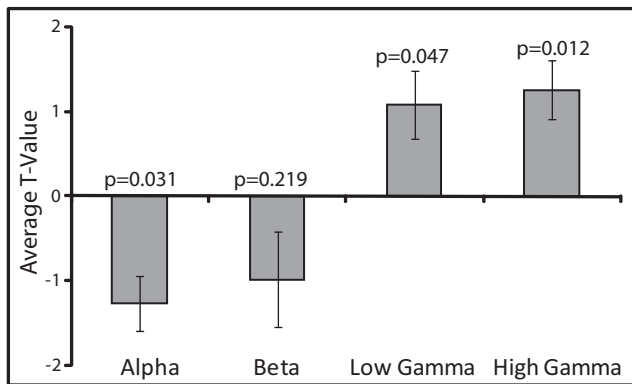


Figure 4. BOLD-EEG Power Coupling for Subjects that Show a Sustained Low-Gamma Band Response

Separate models were estimated for the different frequency bands, for which a design matrix as depicted in Figure 3G was used. The time-frequency analyses of power in the low-gamma range for selected and nonselected subjects are depicted in Figure S3.

pyramidal neurons increased low-frequency power. This finding suggests that interneurons and pyramidal cells play distinct roles in the generation of low- and high-frequency synchronization. Yet, both phenomena certainly involve both neuron types during their physiological generation (Börger and Kopell, 2005; Hasenstaub et al., 2005). Also, local neuronal synchronization phenomena at any frequency are rendered visible for LFP recordings in part when they impinge on pyramidal cells with asymmetric cell shapes, resulting in mesoscopic current fluxes. Some evidence in humans also suggests alpha and high gamma can be dissociated. In a task closely related to our task, larger visual high-gamma power increases were observed with larger contrast, while alpha and beta power remain largely unaltered (Koch et al., 2009).

In our view, our findings of an independent contribution of low- and high-frequency dynamics, together with the converging evidence discussed above, may have substantial implications for our understanding of the BOLD signal. First, our findings indicate that the relationship between BOLD and neurophysiology does not hinge primarily on neuronal dynamics in the gamma frequency range, as recent animal work has suggested (Goense and Logothetis, 2008; Logothetis et al., 2001; Niessing et al., 2005). Our results support the notion that more frequency bands should be taken into account as correlates of the BOLD signal (Kilner et al., 2005; Laufs et al., 2006; Rosa et al., 2010).

Second, our findings contradict the hypothesis that BOLD activation is closely related to a shift in the EEG spectral profile to higher frequencies as a consequence of larger energy dissipation (Kilner et al., 2005). This theory would predict an inverse trial-by-trial coupling between low- and high-frequency power, which is clearly not observed here. We do find the expected

pattern of negative correlations between BOLD and low-frequency power and a positive correlation between BOLD and high-frequency power. At trial-by-trial level the high- and low-power effects are not correlated, however, as would be expected based on this theory.

In a recent article Rosa and colleagues reported evidence for a spectral profile shift in a simultaneous EEG-fMRI experiment (Rosa et al., 2010). However, here only frequencies up to 40 Hz were considered. The high-gamma band effect we observed is of a substantially higher frequency (~60–80 Hz). It is therefore possible that a shift in spectral profile contributes to the BOLD signal, but the high-gamma band effect observed in our study is clearly independent of the effects observed in lower frequency bands and therefore probably independent of the proposed shift in spectral profile. In our data in only a minority of the subjects was a reliable increase in gamma activity around 40 Hz observed, but for these subjects there was a clear trend of a positive relation between low-gamma power and the BOLD signal, which is in line with findings by Mulert et al. (2010). Others, however, have reported a decoupling between gamma power and BOLD in the low-gamma frequency range (Muthukumaraswamy and Singh, 2009). However, because of the limited number of subjects that showed a clear low-gamma band power increase, we were not able to investigate this in further detail.

Third, the independent contributions of low- and high-frequency neuronal dynamics to the BOLD signal imply that simultaneous recording of electrophysiology and hemodynamic activity can potentially dissociate whether an observed BOLD activation or deactivation is related to either low- or high-frequency effects, or a combination of both. In conventional hemodynamic studies it is impossible to make these distinctions. The ability to relate hemodynamic (de)activations to frequency-specific power changes can substantially benefit the interpretation of results obtained by hemodynamic studies, because neuronal activity in different frequency bands has been hypothesized to subservise different functions. For instance, the band-limited gamma effects observed here have been linked to enhanced neural communication (Fries, 2005) while alpha oscillations have been related to functional inhibition (Klimesch et al., 2007).

Several studies have stressed the modulatory effect of slow and infraslow (<0.1 Hz) electrophysiological fluctuations on the amplitude of higher frequencies (He et al., 2010; Monto et al., 2008) and related it to the BOLD signal (He et al., 2008; Nir et al., 2008) and the brain-wide resting-state networks observed in fMRI (Fox and Raichle, 2007). The BOLD-EEG power coherence analysis revealed that indeed the coupling between high-gamma power and BOLD is in part related to fluctuations in a very low-frequency range (<0.02 Hz). For the higher part of the beta band elevated coherence was observed in the high end of the infraslow range (0.5–0.1 Hz). In addition, however, coherent fluctuations in a frequency range close to the trial repetition rate (roughly above 0.12 Hz) were observed in all three

(G) The design matrix that is the basis for the results shown in (C) and (D) and the separate models depicted in (E). The columns of this figure depict the regressors for a single measurement session for a single frequency bin. The first column depicts the EEG power-based regressor for that particular frequency. This regressor is different for each frequency bin. The other regressors model the various parts of the task and potential movement artifacts that are listed on the right in colors that correspond with the boxes grouping the regressors in the design matrix. The design matrix for the single model depicted in (E) only differed in that it included three EEG power-based regressors instead of one.

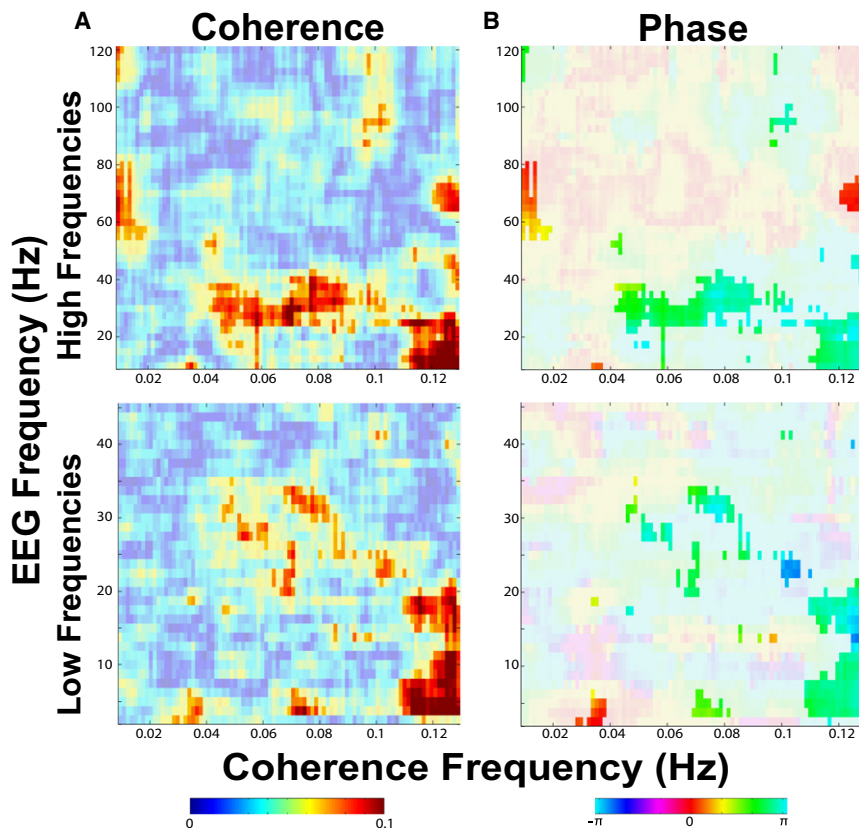


Figure 5. Coherence between EEG Power and the BOLD Signal

For each frequency bin in the EEG spectrum for which the EEG-BOLD correlation was calculated and depicted in Figures 3C and 3D, the coherence between the BOLD signal and the EEG power regressor was calculated after the regressors modeling the task, reaction time, movement effects, and a linear trend (see Figure 3G) were removed by linear regression. The y axis depicts the EEG frequencies and the x axis the frequencies for which the coherence between the EEG power regressor and BOLD was calculated. The coherence values masked at $p = 0.001$ (uncorrected) for both high- and low-frequency ranges are shown in (A). The associated phase of the coherence depicted in (A) is shown in (B). The same mask as in (A) was applied here.

Logothetis, 2008; Logothetis et al., 2001; Niessing et al., 2005), of a strong coupling between hemodynamic responses on the one hand and high-gamma band (60–80 Hz) neuronal synchronization on the other hand. Our results are in line with a recent study that combined NIRS and EEG and that also suggested a BOLD-gamma coupling in humans (Koch et al., 2009). The inference in this study was primarily based on a parametric modulation of both

frequency bands that showed a relation to the BOLD signal (alpha, beta, and gamma). This indicates that for all three frequency bands the EEG-BOLD coupling is (in part) irrespective of fluctuations in the infraslow frequency range. This analysis still leaves open the question of whether fluctuations in the infraslow frequency range contribute directly to the BOLD signal or indirectly through its influence on the strengths of gamma or high-beta oscillations, which cannot be addressed specifically in this experiment.

At first glance, the very low-frequency power-BOLD coupling in the gamma range seems to correspond well with what has been suggested by Nir and colleagues (2008), for example. However, there is a marked difference between the relatively narrow-band gamma component (~20 Hz wide) that is observed in our data and the gamma band power that is locked to the phase of lower frequencies, which has been observed in frequency ranges that can start in the low-gamma range and can go up 200 Hz (He et al., 2010). These wide-band gamma range phenomena are probably not of oscillatory nature (Kayser and Ermentrout, 2010). The narrow-band gamma response in our analysis does suggest an underlying oscillatory process. The effect in the gamma frequency observed here might therefore reflect a different process, as the gamma band process is usually found to be related to infraslow fluctuations.

Concerning the relationship between BOLD and gamma, the combined results of the different analyses presented in this work confirm previous findings from animal work (Goense and

BOLD and gamma, and no trial-by-trial coupling was reported. Our results are also supported by findings from a study with separate intracranial recordings of EEG and fMRI (Lachaux et al., 2007; Zaehle et al., 2009). Studies with simultaneous EEG-fMRI until now only investigated the lower gamma range up to 40 Hz in both tasks (Mulert et al., 2010) as well as in resting-state conditions (Giraud et al., 2007; Mantini et al., 2007). In line with our results, these studies also yielded positive BOLD-gamma correlations. A clear trend for a positive relation between BOLD and gamma power in this frequency range was also found for the subset of subjects that showed a clear increase in power in this range. However, in our study we are also able to show BOLD-gamma coupling in a frequency range up to twice the frequency (80 Hz) reported in previous studies for a region that has been identified as the source region by MEG (Hoogenboom et al., 2006).

In the past studies have reported decoupling between task-induced BOLD changes on the one hand and changes in the gamma power (Muthukumaraswamy and Singh, 2008, 2009), beta power (Stevenson et al., 2011), and intracranially recorded event-related potentials (Huettel et al., 2004). The findings seem at odds with our findings. We think, however, that demonstrating trial-by-trial coupling between electrophysiological signals and the BOLD signal, which is only possible with simultaneous measurements, more directly addresses the issue of how the two modalities are related. In this context, the notion we put forward that there are multiple neural processes that

independently contribute to the changes in the BOLD signal can obscure the ability to observe coupling between electrophysiological and hemodynamic signals that are measured separately; it is not unlikely that the different neural processes that influence the BOLD signal are differentially modulated by the same task manipulations. On the other hand, it cannot be excluded that there is a true decoupling in response to certain task or stimulus manipulations.

In analogy to previous papers on the relationship between BOLD and neuronal oscillations (Logothetis et al., 2001, Niessing et al., 2005), we used the visual system here as an important (and relatively easily accessible) model system. This raises the question, however, of whether our results can be generalized to reflect BOLD-EEG relationships across tasks, brain areas, and cognitive functions. Although we are reporting here only on BOLD-gamma relations in visual cortex, elsewhere it has been extensively argued that gamma is a phenomenon that has been observed across the entire cortex and in response to different tasks and cognitive functions (Fries, 2009). Physiologically, gamma oscillations are probably caused by interactions between pyramidal cells and interneuron (basket) cells and as such, gamma band neuronal synchronization is probably a generic mechanism underlying cortical functioning. For alpha and beta power more empirical data is available showing a negative relationship between power and the BOLD signal in a variety of tasks and regions (Feige et al., 2005; Laufs et al., 2003a, 2003b; Meltzer et al., 2007; Moosmann et al., 2003; Scheeringa et al., 2009; Yuan et al., 2010), although alpha oscillations have been suggested to originate from different combinations of cortical layers in different regions (Bollimunta et al., 2008). For power changes in the beta range, good anatomical correspondence between BOLD changes and power changes has also been observed outside the visual system (Singh et al., 2002; Stevenson et al., 2011; Yuan et al., 2010). Taken together we would predict the BOLD-EEG relationships demonstrated in this article to hold across many different brain areas, tasks, and cognitive functions. Obviously, testing this prediction requires additional empirical work.

In this context, it should also be noted that in the resting-state literature on EEG-BOLD coupling in humans, an intricate picture emerges of relationships between frequency bands and BOLD changes across different areas (e.g., Mantini et al., 2007, Laufs et al., 2006). However, there is one crucial difference between the current approach and these resting-state studies. In order to fully appreciate this difference, one should consider the evidence by Niessing et al. (2005) that the coupling between BOLD and neuronal activity is different when changes in stimulation parameters (such as contrast) are used as the source of variance in both signals, compared to the coupling observed during spontaneous fluctuations around the average level of, e.g., gamma or BOLD. In the data from Niessing and colleagues the fluctuations around the average BOLD response gave the most specific coupling between BOLD and neuronal activity (here LFPs). Exactly for this reason, our present analyses focus on spontaneous trial-by-trial fluctuations around the mean EEG power changes and correlate this with the trial-by-trial fluctuations in the BOLD signal. Furthermore, the very strong (more than 500% increase relative to baseline in some subjects),

high-frequency, narrow-band gamma oscillations we observe in our paradigm have not been reported yet in resting-state EEG and it is questionable whether this phenomenon can actually be observed in EEG or MEG originating from brain regions that are “at rest.”

In conclusion, our data provide the most direct evidence yet that the coupling between BOLD and high-gamma band oscillations in animal work also holds in humans performing a cognitive task. More importantly, our data suggest that at least two independent neurophysiological mechanisms contribute to the generation of the BOLD signal that can be observed during cognitive neuroscientific experiments in humans: (1) a mechanism related to high-frequency (high-gamma band) neuronal synchronization, which correlates positively with BOLD signal changes and (2) a mechanism reflected in low-frequency (alpha and beta bands) neuronal synchronization, which correlates negatively with BOLD signal changes. As such, the present work provides a step forward in understanding the electrophysiological underpinnings of cognition-related hemodynamic responses in humans.

EXPERIMENTAL PROCEDURES

Subjects

Twenty right-handed subjects (13 female, 7 male, mean age 24 years, range 19–31 years) without a history of known psychiatric or neurological disorders participated in the simultaneous EEG/fMRI session. All had normal or corrected-to-normal vision. Before the start of the experiment, written informed consent was obtained from each subject. The experiment was approved by a local ethical committee (CMO region Arnhem / Nijmegen).

Experimental Paradigm

It has been established that neuronal synchronization in the gamma frequency range is associated, among others, with attentional processes, most notably in the visual system (Bichot et al., 2005; Fries et al., 2001; Lakatos et al., 2008). Therefore, subjects engaged in a visual attention task that is known to elicit strong, long-lasting (up to several seconds), and narrow-band gamma activity in the MEG (Hoogenboom et al., 2006). In this task, subjects attend to circular, inward-moving gratings and are asked to detect a change in inward speed. In the lower frequency bands this task induces strong and long-lasting decreases in alpha and beta power. Trials were triggered by the onset of an fMRI volume and occurred every two volumes. fMRI images were recorded in 330 ms, followed by a 3300 ms scan-free period. This scan-free period allowed us to collect EEG data that were free of gradient artifacts during the visual stimulation interval. In total, four blocks of 100 trials (20 of each trial length) were administered. One block had a length of approximately 12 min, 30 s. The experimental paradigm is illustrated in Figure 1 and described in full in the Supplemental Experimental Procedures.

MRI Data Acquisition

Functional and structural MRI data were acquired by using a 3.0-T whole-body MRI scanner (Siemens Magnetom Trio Tim, Siemens, Erlangen, Germany). A custom-built eight channel array (Stark Contrast, MRI Coils, Erlangen, Germany; Barth and Norris, 2007) covering the occipital cortex was used to record the functional images. One volume was acquired in 330 ms, followed by a 3300 ms gap allowing for gradient-free EEG recording (see Figure 1). After the four functional runs, an anatomical image was acquired. MRI data acquisition is described in more detail in the Supplemental Experimental Procedures.

EEG Data Acquisition

EEG data was recorded with a custom-made MRI-compatible cap equipped with carbon-wired Ag/AgCl electrodes (Easycap, Herrsching-Breitbrunn,

Germany). Data were recorded from 29 scalp sites selected from the 128 channel international 10-10 system by using an MRI-compatible EEG amplifier (BrainAmp MR plus, Brainproducts, Munich, Germany). The placement of the electrodes was focused over posterior regions, so that signals coming from visual regions could be recorded with greater accuracy. The reference electrode during recording was placed at Cz. The exact details of the EEG data acquisition can be found in the [Supplemental Experimental Procedures](#).

fMRI Data Analysis

For getting single subject fMRI activations related to visual stimulation, fMRI data was preprocessed and analyzed in SPM5 (Wellcome Department of Imaging Neuroscience, London, UK; see <http://www.fil.ion.ucl.ac.uk/spm>) in a conventional way by using box-car regressors convolved with the canonical hemodynamic response function. For each single subject, all voxels with a *t*-value greater than 10 formed a region of interest for the integrated EEG-fMRI analysis (see the right-hand panels of [Figure S1](#) for the resulting BOLD activation maps for each single subject). For more details, see the [Supplemental Experimental Procedures](#).

EEG Data: Time-Frequency Analysis

Downsampling, re-referencing, trial extraction, and artifact rejection of the EEG data were carried out in Vision Analyzer (Brainproducts GmbH, Germany). The full details on the preprocessing of the EEG data are described in the [Supplemental Experimental Procedures](#). Further analysis of the EEG data was carried out in Fieldtrip (Oostenveld et al., 2011). Time-frequency analysis was carried out by using a multitaper approach (Mitra and Pesaran, 1999). In order to optimize the trade-off between time and frequency resolution, we carried out separate analyses for a lower frequency window (2.5–45 Hz) and a higher frequency window (10–120 Hz). For the lower frequencies, the power was estimated for windows of 0.8 s length moved across the data in steps of 50 ms. This resulted in a frequency resolution of 1.25 Hz, and the use of three tapers resulted in a spectral smoothing of ± 2.5 Hz. For the higher frequencies, the power was estimated for windows of 0.4 s length moved across the data in steps of 50 ms. This resulted in a frequency resolution of 2.5 Hz, and the use of seven tapers resulted in a spectral smoothing of ± 10 Hz.

An initial analysis was carried out at channel level, revealing a similar sustained gamma band response as that described by Hoogenboom and colleagues (2006) for some of the subjects. However, because of EMG contamination and artifacts caused by the MR recording environment, data for most subjects was too noisy to observe this effect directly.

EEG Data: ICA-Based Denoising

To denoise the data, we used an ICA approach adapted from a similar approach applied by Debener et al. (2005) with the extended infomax algorithm (Lee et al., 1999) as implemented in EEGLab 5.03 (Delorme and Makeig, 2004). In this approach, ICA unmixing weights were estimated on individually adjusted gamma-band-filtered EEG data. These unmixing weights thus obtained were applied on the unfiltered EEG data. For each subject the components that showed sustained gamma band response in time course were projected back to channel level (1–5 components for each subject). Finally, these channel-level data were again subjected to a time-frequency analysis, separately for the lower and the higher frequency windows, as described in the previous section. The results of this analysis constitute the basis for the construction of regressors that were used in the integrated EEG fMRI analysis.

This strategy proved to be the best strategy to denoise the EEG data across the different frequency bands that have been reported before (Hoogenboom et al., 2006; Koch et al., 2009). For comparison, this ICA denoising strategy analysis was repeated for 30 Hz low-pass-filtered data. Although similar effects are observed in the alpha and beta bands, this strategy proved to be inadequate to optimally denoise the EEG in the gamma band. The results of this analysis are presented in [Figure S2](#). The full details of the ICA denoising strategy are described in the [Supplemental Experimental Procedures](#).

Integrated EEG and fMRI Analysis: Regressor Construction

For each subject, the EEG channel with the maximal gamma power increase in the average spectrum over trials (defined as the average increase across time

points and trials during visual stimulation in the 55–85 Hz band, relative to a 200 ms previsual stimulation baseline) was selected. In addition, all the channels were selected that showed a gamma power increase of at least 25% of the gamma power increase of that channel. These selected channels were used for the construction of regressors for both the low and the high frequencies.

Next, for each frequency bin, considering the analysis of the lower and higher frequency windows separately, EEG-based regressors were constructed as follows. For each single trial, the power time course during the stimulation interval was averaged across the selected channels (no baseline correction). These power time courses were concatenated into one time series. This time series was subsequently convolved with the canonical hemodynamic response function as implemented in SPM5 and downsampled to one value for each scan. This resulted in one EEG-based regressor for each frequency bin, both in the analysis on the lower frequency window and in the analysis on the higher frequency window.

For the ICA denoising based on low-pass-filtered data represented in [Figure S2](#), regressor construction was similar, with the only exception being the channel selection. For this channels were included where the power decrease in the 8–25 Hz range was at least 25% of the maximum power decrease on any channel. Within this analysis the same selected channels were again used for the construction of regressors for both the low and the high frequencies.

Integrated EEG and fMRI Analysis: Statistical Models

The region of interest data obtained from single-subject stimulation versus baseline contrast were analyzed in a general linear model context by using frequency-specific design matrices. Separate models were run for each frequency bin (1.25 Hz bins for the low-frequency range, 2.5 Hz bins for the high-frequency range). For each frequency bin, the regressor modeling the single-trial power estimates of that frequency bin was included in the design matrix. All the other regressors in the design matrix were the same for all frequency bins. These included (1) five HRF-convolved box-car regressors (one for each trial length) that account for the main effect of visual stimulation on the BOLD signal, (2) five regressors modeling the button press and feedback (one for each trial length)-related BOLD activity, (3) four regressors modeling the reaction time as a parametric modulation (one for each trial type with a speed change), (4) a regressor that modeled the behaviorally incorrect trials, (5) the six realignment parameters used to control for possible movement artifacts, and (6) one regressor accounting for a linear trend. A graphical representation of the design matrix is shown in [Figure 3G](#). The four runs from each subject were modeled with separate regressors.

In the context of the regressors modeling the task and the parametric regressors modeling the reaction time, the frequency-specific EEG power regressor accounts for the relation between single-trial variations in EEG power and the BOLD signal for the EEG frequency in question. At the single-subject level, for each frequency, the relation between the EEG power regressors and the BOLD signal is assessed by a single-sample *t*-contrast of these regressors against zero. At group level we averaged these *t*-values over subjects and tested whether they significantly differed from zero. We chose *t*-values because the beta regression weights critically depend on the scale of the power fluctuations, which can differ by orders of magnitude between frequencies and subjects. Because all sessions for all subjects had the same number of regressors, the *t*-values do not differ between subjects a priori.

Analysis with EEG power regressors based on ICA applied on low-pass-filtered data was carried out in the same way. The results are depicted in [Figure S2](#).

The results of the analysis detailed above yielded significant negative correlations between alpha and beta power fluctuations and BOLD and a positive correlation between gamma power fluctuations and BOLD. This raised the question of whether this was due to one or more underlying processes that correlate with the BOLD signal. To investigate this, we first ran another GLM in which we included three regressors modeling the trial-by-trial variability in these three frequency bands. For comparison, we computed three separate models including only one of the EEG power-based regressors. For each frequency band, the regressor was based on the average of the power across the frequency bins that was part of the significant cluster in the EEG-BOLD correlation. This analysis evaluates whether the regressors can account for unique variance in the BOLD signal. As a second step, the partial correlations

between these three regressors were computed, separating out the regressors modeling the main effect of visual stimulation and the response time.

In addition to a high-gamma band response, a substantial minority of the subjects also show a clear low-gamma power increase in response in the low-gamma range (30–45 Hz). In a separate analysis we explore the relation between this low-gamma response. First we selected seven subjects that had a clear sustained increase in the lower gamma range (see [Figure S3](#) for the time-frequency representations for all subjects). Second we formed a single regressor for the low-gamma response for each subject. The basis for this regressor was formed by the subject-specific single-trial low-gamma power responses. These single-trial responses were calculated by averaging over the frequency bin showing the maximal relative low-gamma power increase (compared to baseline) and the bin below and above. Further regressor construction and statistical models were similar to those described above for the other frequency bands.

Coherence between BOLD and EEG Power Regressors

To investigate whether infraslow fluctuations are related to the trial-by-trial coupling we observed in the alpha, beta, and gamma ranges we calculated the coherence ([Baker et al., 1997](#); [Rosenberg et al., 1989](#)) between the EEG power regressors and the BOLD signal. This analysis was carried out for each frequency bin in the EEG-BOLD correlational analysis. As a first step, for each session of each subject, the influence the task, RT, and realignment regressors have on both the BOLD signal and each EEG power regressor was removed by linear regression. The power spectrum was calculated for the residues of this regression for both BOLD and EEG power regressors by means of a multitaper approach with a frequency smoothing of ± 0.0095 Hz, resulting in 13 tapers. The coherence between BOLD and trial-by-trial EEG power fluctuations was calculated over all sessions of all the subjects (80 in total). Each session has a length of 740.52 s, resulting in a frequency resolution of 0.0014 Hz. The TR of 3.63 s restricts the analysis to frequencies up to 0.1377 Hz. Because we use a frequency smoothing of 0.0095 Hz, coherence was estimated for frequency bins between 0.0095 and 0.1282 Hz. For statistical inference the coherence values were z-transformed ([Rosenberg et al., 1989](#)). The coherence values were thresholded at $p = 0.001$.

Inferential Statistics

Significance at the group level of the EEG power changes relative to baseline ([Figures 3A and 3B](#)) and of the BOLD-EEG power relation ([Figures 3C and 3D](#)) was evaluated by a cluster-based randomization procedure ([Maris and Oostenveld, 2007](#)). This effectively controls the Type-1 error rate in a situation involving multiple comparisons (here: all the individual frequency bins). This procedure allows for user-defined test statistics tailored to the effect of interest within the framework of a cluster-based randomization test. For the BOLD-EEG power relation, our test statistic was a single-sample t test against zero of the averaged t-value over subjects (giving uncorrected p-values). All data points that do not exceed a preset significance level (here 5%) are zeroed. Clusters of adjacent nonzero frequency points were computed and for each cluster, a cluster-level test statistic is calculated by taking the sum of all the individual t-statistics within that cluster. This statistic was entered in the cluster-based randomization procedure. This same procedure was also used to test the difference of the EEG power from baseline. The test statistic was a single-sample t test of the log-transformed relative power compared to baseline (the 200 ms prestimulation interval). The above procedures were applied separately to the analyses of the lower and the higher frequencies.

The Wilcoxon ranked sign test was used to test deviations from zero at group level ([Wilcoxon, 1945](#)) for the models investigating the dependency between regressors and the pairwise partial correlation between regressors and for the analysis focused on the low-gamma band response.

SUPPLEMENTAL INFORMATION

Supplemental Information includes Supplemental Experimental Procedures and three figures and can be found with this article online at [doi:10.1016/j.neuron.2010.11.044](https://doi.org/10.1016/j.neuron.2010.11.044).

ACKNOWLEDGMENTS

We would like to thank Nienke Hoogenboom for her help in programming the experimental paradigm. This work was supported by a grant from The Netherlands Organisation for Scientific Research (NWO, grant number 400-03-277). I.G. was supported by the BMBF Grant 01GQ0705 (Bernstein Group for Computational Neuroscience Bremen).

Accepted: November 23, 2010

Published: February 9, 2011

REFERENCES

- Baker, S.N., Olivier, E., and Lemon, R.N. (1997). Coherent oscillations in monkey motor cortex and hand muscle EMG show task-dependent modulation. *J. Physiol.* *501*, 225–241.
- Barth, M., and Norris, D.G. (2007). Very high-resolution three-dimensional functional MRI of the human visual cortex with elimination of large venous vessels. *NMR Biomed.* *20*, 477–484.
- Bichot, N.P., Rossi, A.F., and Desimone, R. (2005). Parallel and serial neural mechanisms for visual search in macaque area V4. *Science* *308*, 529–534.
- Bollimunta, A., Chen, Y., Schroeder, C.E., and Ding, M. (2008). Neuronal mechanisms of cortical alpha oscillations in awake-behaving macaques. *J. Neurosci.* *28*, 9976–9988.
- Börgers, C., and Kopell, N. (2005). Effects of noisy drive on rhythms in networks of excitatory and inhibitory neurons. *Neural Comput.* *17*, 557–608.
- Cardin, J.A., Carlén, M., Meletis, K., Knoblich, U., Zhang, F., Deisseroth, K., Tsai, L.H., and Moore, C.I. (2009). Driving fast-spiking cells induces gamma rhythm and controls sensory responses. *Nature* *459*, 663–667.
- Debener, S., Ullsperger, M., Siegel, M., Fiehler, K., von Cramon, D.Y., and Engel, A.K. (2005). Trial-by-trial coupling of concurrent electroencephalogram and functional magnetic resonance imaging identifies the dynamics of performance monitoring. *J. Neurosci.* *25*, 11730–11737.
- Delorme, A., and Makeig, S. (2004). EEGLAB: An open source toolbox for analysis of single-trial EEG dynamics including independent component analysis. *J. Neurosci. Methods* *134*, 9–21.
- Feige, B., Scheffler, K., Esposito, F., Di Salle, F., Hennig, J., and Seifritz, E. (2005). Cortical and subcortical correlates of electroencephalographic alpha rhythm modulation. *J. Neurophysiol.* *93*, 2864–2872.
- Fries, P. (2005). A mechanism for cognitive dynamics: Neuronal communication through neuronal coherence. *Trends Cogn. Sci. (Regul. Ed.)* *9*, 474–480.
- Fries, P. (2009). Neuronal gamma-band synchronization as a fundamental process in cortical computation. *Annu. Rev. Neurosci.* *32*, 209–224.
- Fries, P., Reynolds, J.H., Rorie, A.E., and Desimone, R. (2001). Modulation of oscillatory neuronal synchronization by selective visual attention. *Science* *291*, 1560–1563.
- Fries, P., Scheeringa, R., and Oostenveld, R. (2008). Finding gamma. *Neuron* *58*, 303–305.
- Fox, M.D., and Raichle, M.E. (2007). Spontaneous fluctuations in brain activity observed with functional magnetic resonance imaging. *Nat. Rev. Neurosci.* *8*, 700–711.
- Giraud, A.L., Kleinschmidt, A., Poeppel, D., Lund, T.E., Frackowiak, R.S., and Laufs, H. (2007). Endogenous cortical rhythms determine cerebral specialization for speech perception and production. *Neuron* *56*, 1127–1134.
- Goense, J.B., and Logothetis, N.K. (2008). Neurophysiology of the BOLD fMRI signal in awake monkeys. *Curr. Biol.* *18*, 631–640.
- Goldman, R.I., Stern, J.M., Engel, J., Jr., and Cohen, M.S. (2002). Simultaneous EEG and fMRI of the alpha rhythm. *Neuroreport* *13*, 2487–2492.
- Hall, S.D., Holliday, I.E., Hillebrand, A., Singh, K.D., Furlong, P.L., Hadjipapas, A., and Barnes, G.R. (2005). The missing link: Analogous human and primate cortical gamma oscillations. *Neuroimage* *26*, 13–17.

- Hasenstaub, A., Shu, Y., Haider, B., Kraushaar, U., Duque, A., and McCormick, D.A. (2005). Inhibitory postsynaptic potentials carry synchronized frequency information in active cortical networks. *Neuron* 47, 423–435.
- He, B.J., Snyder, A.Z., Zempel, J.M., Smyth, M.D., and Raichle, M.E. (2008). Electrophysiological correlates of the brain's intrinsic large-scale functional architecture. *Proc. Natl. Acad. Sci. USA* 105, 16039–16044.
- He, B.J., Zempel, J.M., Snyder, A.Z., and Raichle, M.E. (2010). The temporal structures and functional significance of scale-free brain activity. *Neuron* 66, 353–369.
- Hoogenboom, N., Schoffelen, J.M., Oostenveld, R., Parkes, L.M., and Fries, P. (2006). Localizing human visual gamma-band activity in frequency, time and space. *Neuroimage* 29, 764–773.
- Huettel, S.A., McKeown, M.J., Song, A.W., Hart, S., Spencer, D.D., Allison, T., and McCarthy, G. (2004). Linking hemodynamic and electrophysiological measures of brain activity: Evidence from functional MRI and intracranial field potentials. *Cereb. Cortex* 14, 165–173.
- Jokisch, D., and Jensen, O. (2007). Modulation of gamma and alpha activity during a working memory task engaging the dorsal or ventral stream. *J. Neurosci.* 27, 3244–3251.
- Kayser, C., and Ermentrout, B. (2010). Complex times for earthquakes, stocks, and the brain's activity. *Neuron* 66, 329–331.
- Kilner, J.M., Mattout, J., Henson, R., and Friston, K.J. (2005). Hemodynamic correlates of EEG: A heuristic. *Neuroimage* 28, 280–286.
- Klimesch, W., Doppelmayr, M., Russegger, H., Pachinger, T., and Schwaiger, J. (1998). Induced alpha band power changes in the human EEG and attention. *Neurosci. Lett.* 244, 73–76.
- Klimesch, W., Sauseng, P., and Hanslmayr, S. (2007). EEG alpha oscillations: The inhibition-timing hypothesis. *Brain Res. Rev.* 53, 63–88.
- Koch, S.P., Werner, P., Steinbrink, J., Fries, P., and Obrig, H. (2009). Stimulus-induced and state-dependent sustained gamma activity is tightly coupled to the hemodynamic response in humans. *J. Neurosci.* 29, 13962–13970.
- Lachaux, J.P., Fonlupt, P., Kahane, P., Minotti, L., Hoffmann, D., Bertrand, O., and Bacia, M. (2007). Relationship between task-related gamma oscillations and BOLD signal: New insights from combined fMRI and intracranial EEG. *Hum. Brain Mapp.* 28, 1368–1375.
- Lakatos, P., Karmos, G., Mehta, A.D., Ulbert, I., and Schroeder, C.E. (2008). Entrainment of neuronal oscillations as a mechanism of attentional selection. *Science* 320, 110–113.
- Laufs, H., Holt, J.L., Elfont, R., Krams, M., Paul, J.S., Krakow, K., and Kleinschmidt, A. (2006). Where the BOLD signal goes when alpha EEG leaves. *Neuroimage* 31, 1408–1418.
- Laufs, H., Kleinschmidt, A., Beyerle, A., Eger, E., Salek-Haddadi, A., Preibisch, C., and Krakow, K. (2003a). EEG-correlated fMRI of human alpha activity. *Neuroimage* 19, 1463–1476.
- Laufs, H., Krakow, K., Sterzer, P., Eger, E., Beyerle, A., Salek-Haddadi, A., and Kleinschmidt, A. (2003b). Electroencephalographic signatures of attentional and cognitive default modes in spontaneous brain activity fluctuations at rest. *Proc. Natl. Acad. Sci. USA* 100, 11053–11058.
- Lee, T.W., Girolami, M., and Sejnowski, T.J. (1999). Independent component analysis using an extended infomax algorithm for mixed subgaussian and supergaussian sources. *Neural Comput.* 11, 417–441.
- Logothetis, N.K. (2008). What we can do and what we cannot do with fMRI. *Nature* 453, 869–878.
- Logothetis, N.K., Pauls, J., Augath, M., Trinath, T., and Oeltermann, A. (2001). Neurophysiological investigation of the basis of the fMRI signal. *Nature* 412, 150–157.
- Mantini, D., Perrucci, M.G., Del Gratta, C., Romani, G.L., and Corbetta, M. (2007). Electrophysiological signatures of resting state networks in the human brain. *Proc. Natl. Acad. Sci. USA* 104, 13170–13175.
- Maris, E., and Oostenveld, R. (2007). Nonparametric statistical testing of EEG- and MEG-data. *J. Neurosci. Methods* 164, 177–190.
- Meltzer, J.A., Negishi, M., Mayes, L.C., and Constable, R.T. (2007). Individual differences in EEG theta and alpha dynamics during working memory correlate with fMRI responses across subjects. *Clin. Neurophysiol.* 118, 2419–2436.
- Mitra, P.P., and Pesaran, B. (1999). Analysis of dynamic brain imaging data. *Biophys. J.* 76, 691–708.
- Monto, S., Palva, S., Voipio, J., and Palva, J.M. (2008). Very slow EEG fluctuations predict the dynamics of stimulus detection and oscillation amplitudes in humans. *J. Neurosci.* 28, 8268–8272.
- Moosmann, M., Ritter, P., Krastel, I., Brink, A., Thees, S., Blankenburg, F., Taskin, B., Obrig, H., and Villringer, A. (2003). Correlates of alpha rhythm in functional magnetic resonance imaging and near infrared spectroscopy. *Neuroimage* 20, 145–158.
- Mukamel, R., Gelbard, H., Arieli, A., Hasson, U., Fried, I., and Malach, R. (2005). Coupling between neuronal firing, field potentials, and fMRI in human auditory cortex. *Science* 309, 951–954.
- Mulert, C., Leicht, G., Hepp, P., Kirsch, V., Karch, S., Pogarell, O., Reiser, M., Hegerl, U., Jäger, L., Moller, H.J., and McCarley, R.W. (2010). Single-trial coupling of the gamma-band response and the corresponding BOLD signal. *Neuroimage* 49, 2238–2247.
- Muthukumaraswamy, S.D., and Singh, K.D. (2009). Functional decoupling of BOLD and gamma-band amplitudes in human primary visual cortex. *Hum. Brain Mapp.* 30, 2000–2007.
- Muthukumaraswamy, S.D., and Singh, K.D. (2008). Spatiotemporal frequency tuning of BOLD and gamma band MEG responses compared in primary visual cortex. *Neuroimage* 40, 1552–1560.
- Niessing, J., Ebisch, B., Schmidt, K.E., Niessing, M., Singer, W., and Galuske, R.A. (2005). Hemodynamic signals correlate tightly with synchronized gamma oscillations. *Science* 309, 948–951.
- Nir, Y., Mukamel, R., Dinstein, I., Privman, E., Harel, M., Fisch, L., Gelbard-Sagiv, H., Kipervasser, S., Andelman, F., Neufeld, M.Y., et al. (2008). Interhemispheric correlations of slow spontaneous neuronal fluctuations revealed in human sensory cortex. *Nat. Neurosci.* 11, 1100–1108.
- Oostenveld, R., Fries, P., Maris, E., and Schoffelen, J.M. (2011). FieldTrip: Open source software for advanced analysis of MEG, EEG, and invasive electrophysiological data. *Comput. Intell. Neurosci.* 2011, 156869.
- Palva, S., and Palva, J.M. (2007). New vistas for alpha-frequency band oscillations. *Trends Neurosci.* 30, 150–158.
- Pfurtscheller, G., Stancák, A., Jr., and Neuper, C. (1996a). Event-related synchronization (ERS) in the alpha band—an electrophysiological correlate of cortical idling: A review. *Int. J. Psychophysiol.* 24, 39–46.
- Pfurtscheller, G., Stancák, A., Jr., and Neuper, C. (1996b). Post-movement beta synchronization. A correlate of an idling motor area? *Electroencephalogr. Clin. Neurophysiol.* 98, 281–293.
- Posthuma, D., Neale, M.C., Boomsma, D.I., and de Geus, E.J. (2001). Are smarter brains running faster? Heritability of alpha peak frequency, IQ, and their interrelation. *Behav. Genet.* 31, 567–579.
- Rosa, M.J., Kilner, J., Blankenburg, F., Josephs, O., and Penny, W. (2010). Estimating the transfer function from neuronal activity to BOLD using simultaneous EEG-fMRI. *Neuroimage* 49, 1496–1509.
- Rosenberg, J.R., Amjad, A.M., Breeze, P., Brillinger, D.R., and Halliday, D.M. (1989). The Fourier approach to the identification of functional coupling between neuronal spike trains. *Prog. Biophys. Mol. Biol.* 53, 1–31.
- Scheeringa, R., Bastiaansen, M.C., Petersson, K.M., Oostenveld, R., Norris, D.G., and Hagoort, P. (2008). Frontal theta EEG activity correlates negatively with the default mode network in resting state. *Int. J. Psychophysiol.* 67, 242–251.
- Scheeringa, R., Petersson, K.M., Oostenveld, R., Norris, D.G., Hagoort, P., and Bastiaansen, M.C. (2009). Trial-by-trial coupling between EEG and BOLD identifies networks related to alpha and theta EEG power increases during working memory maintenance. *Neuroimage* 44, 1224–1238.

Singh, K.D., Barnes, G.R., Hillebrand, A., Forde, E.M., and Williams, A.L. (2002). Task-related changes in cortical synchronization are spatially coincident with the hemodynamic response. *Neuroimage* 16, 103–114.

Stevenson, C.M., Brookes, M.J., and Morris, P.G. (2011). β -Band correlates of the fMRI BOLD response. *Hum. Brain Mapp.* 32, 182–197.

Wilcoxon, F. (1945). Individual comparisons by ranking methods. *Biometrics* 1, 80–83.

Yuan, H., Liu, T., Szarkowski, R., Rios, C., Ashe, J., and He, B. (2010). Negative covariation between task-related responses in alpha/beta-band activity and BOLD in human sensorimotor cortex: An EEG and fMRI study of motor imagery and movements. *Neuroimage* 49, 2596–2606.

Zaehle, T., Fründ, I., Schadow, J., Thärig, S., Schoenfeld, M.A., and Herman, C.S. (2009). Inter- and intra-individual covariations of hemodynamic and oscillatory gamma responses in the human cortex. *Front Hum. Neurosci.* 3, 8.